Analytical Methods

PAPER

View Article Online
View Journal | View Issue

Published on 22 September 2015. Downloaded by Michigan State University on 21/01/2016 07:20:08.

Cite this: *Anal. Methods*, 2015, 7, 9237

Synthesis and characterization of a magnetic molecularly imprinted polymer for the selective extraction of nicotine and cotinine from urine samples followed by GC-MS analysis

Lidiane Silva Franqui,[a] Mariane Gonçalves Santos,[a] Luciano Sindra Virtuoso,[b] Patrícia Penido Maia[a] and Eduardo Costa Figueiredo*[a]

Received 12th June 2015
Accepted 19th September 2015

DOI: 10.1039/c5ay01522g

www.rsc.org/methods

A magnetic molecularly imprinted polymer (MMIP) was synthesized, characterized and used in the selective extraction of nicotine and cotinine from urine samples, followed by GC-MS analysis. Fe_3O_4 nanoparticles were prepared by the co-precipitation method, silanized/stabilized with tetraethyl orthosilicate and functionalized with 3-(trimethoxysilyl)propyl methacrylate. The MMIP was prepared on the magnetic nanoparticle surface, using nicotine as the template and methacrylic acid as the functional monomer. The material was characterized by scanning electron microscopy, atomic force microscopy, Fourier transform infrared spectroscopy, energy dispersive X-ray spectrometry and thermogravimetry, where all the synthesis steps were confirmed. The nanoparticles were used in the dispersive solid phase extraction of nicotine and cotinine from human urine samples, and the extracts were analyzed by GC-MS. The analytical curves ranged from 0.1 to 3.0 mg L^{-1} ($r > 0.99$), with a limit of quantification (LOQ) of 0.1 mg L^{-1} for both analytes. The intra- and inter-day precisions were less than 20% for the LOQ and less than 15% for the other points; whereas the intra- and inter-day accuracies were within ±9%. The method was successfully employed to analyze nicotine and cotinine from four real smokers' urine samples.

Introduction

Currently, analytical chemistry is in a very advanced stage in terms of sophisticated equipment availability, for substance separation, identification and quantification. However, despite these advances, in some cases, direct analysis is not possible, because most of the samples have complex matrices with a large number of interferents, which can compromise the precision and accuracy of the used methods, as well as harm the equipment. Thus, the sample preparation stage is critical in order to obtain reliable results and has received great attention recently.[1]

The need to analyze complex samples on a large scale stimulates the exploration of faster, simpler and more selective sample preparation methods,[2] and this led to a great evolution in the development of new selective techniques, such as those based on the use of molecularly imprinted polymers (MIPs).[3]

MIPs are synthetic polymeric materials that have specific cavities for a target molecule, involving a retention mechanism based on molecular recognition. Besides the possibility to prepare sorbents with predetermined selectivity,[4] MIPs have additional advantages such as ease and low cost of synthesis, chemical, physical and thermal stabilities and the possibility to be used for a wide range of target molecules. Thus, polymers have been widely used in analytical techniques, mainly as selective sorbents in solid phase extraction (SPE).[3,5]

Despite the advantages of the conventional molecularly imprinted solid phase extraction (MISPE) in cartridges, some drawbacks of this technique can be emphasized, such as its poor mass transfer, low binding capacity and slow binding kinetics.[6] Hence, a new modality of MIPs, denominated magnetic molecularly imprinted polymers (MMIPs),[7] has received great attention in order to overcome these drawbacks. MMIPs are magnetic nanoparticles covered with MIPs, resulting in a magnetically susceptible selective material. This sorbent can be added directly into the sample, being afterwards recovered by using an external magnet. The obstruction of conventional SPE cartridges, caused by the sample matrix, is avoided,[7,8] and the pretreatment time is reduced, because of the exposed bigger surface area, improving the binding kinetics and capacity. For example, a sensitive method based on MMIPs was developed by Chen *et al.*[9] to extract tetracycline antibiotics from tissue and egg samples. When compared with the molecularly imprinted solid phase microextraction method (MIP-SPME),[10] the MMIP provided a lower limit of detection (LOD) and higher precision (LOD

[a]*Toxicants and Drugs Analysis Laboratory, Faculty of Pharmaceutical Sciences, Federal University of Alfenas – Unifal-MG, 700 Gabriel Monteiro da Silva street, 37130-000, Alfenas, MG, Brazil. E-mail: eduardocfig@yahoo.com.br; Fax: +55 35 3299 1067; Tel: +55 35 3299 1342*

[b]*Colloid Chemistry Group, Chemistry Institute, Federal University of Alfenas – Unifal-MG, 700 Gabriel Monteiro da Silva street, 37130-000, Alfenas, MG, Brazil*

Published on 22 September 2015. Downloaded by Michigan State University on 21/01/2016 07:20:08.

0.06–0.19 ng g^{-1} and RSD 3.4–5.8% for MMIPs; LOD 1.5–3.5 ng g^{-1} and RSD 2.9–12.3% for MIP-SPME). Moreover, the molecularly imprinted solid phase extraction method (MIP-SPE)[11] presented extraction recoveries of about 69%, whereas in the MMIP method the recoveries were >93%. In another study, Zhang *et al.*[12] synthesized a MMIP to extract sterols from complicated biological samples. With this MMIP, they obtained LOD values of about 1.2 and 1.1 μg L^{-1} for stigmasterol and β-sitosterol from serum samples, respectively, which are lower than 17 and 31 μg L^{-1} obtained by conventional solid phase extraction (SPE),[13] and 7.5 and 13 ng mL^{-1} obtained by online SPE,[14] for the same analytes and samples. Additionally, MMIPs have been used to extract several analytes from different samples like herbal medicines,[15–17] water,[18–20] urine,[21,22] fruits,[12,23] honey,[24] egg,[25] milk,[26] wine,[27] poultry feed,[28] serum,[12] mushrooms,[12] soil,[29] soybean,[29] millet,[29] plant tissues,[30] pork and pig liver.[31]

Nowadays, it is common knowledge that smoking is among the leading preventable causes of morbidity and mortality worldwide, being considered as the main cause of lung cancer and an important factor for cardiovascular and chronic pulmonary inflammatory diseases, among other conditions.[32] More than 4000 compounds have been isolated and identified in tobacco smoke, of which more than 20 are alkaloids.[33] Nicotine is the most abundant pharmacologically active alkaloid in tobacco (98% of the total alkaloids) being responsible for its dependency. Furthermore, nicotine is a highly potent toxic agent,[34] with a primarily hepatic biotransformation and a half-life of about 2 h. The main product of nicotine biotransformation is cotinine, and because of its high half-life, it can be determined in different biological fluids, for several days after exposure to tobacco smoke.[33,35] Thus, nicotine and cotinine have been widely used as biological markers to determine smoking habits.

Therefore, MMIPs show up as promising tools for use in complex sample preparation techniques. In this sense, this study is aimed to synthesize a MMIP for the extraction of nicotine and cotinine from urine for the purpose of monitoring exposure to tobacco smoke.

Experimental

Chemicals and samples

HPLC grade methanol and acetonitrile were purchased from Sigma-Aldrich® (Steinheim, Germany). Nicotine and cotinine stock solutions (both from Sigma-Aldrich®, Steinheim, Germany) were prepared at a concentration of 1.0 mg mL^{-1}, in HPLC grade methanol, placed in amber flasks and stored at −18 °C for up to 30 days. Ferric chloride ($FeCl_3 \cdot 6H_2O$), ferrous chloride ($FeCl_2 \cdot 4H_2O$), 3-(methacryloxyl)propyl trimethoxysilane (MPS), tetraethyl orthosilicate (TEOS), methacrylic acid (MAA), ethylene glycol dimethacrylate (EGDMA) and 4,4′-azobis(4-cyanovaleric acid) (ABCVA) (all from Sigma-Aldrich®, Steinheim, Germany) were used in the MMIP synthesis. Sodium dihydrogen phosphate ($NaH_2PO_4 \cdot H_2O$) and disodium hydrogen phosphate (Na_2HPO_4) were obtained from Cinética Química Ltda (São Paulo, Brazil) and Vetec® (Rio de Janeiro, Brazil), respectively. Ammonium hydroxide (28%, v/v) and 2-propanol were both obtained from Isofar® (Rio de Janeiro, Brazil). Hydrochloric and acetic acids were purchased from Furlab® (São Paulo, Brazil) and Êxodo Científica (São Paulo, Brazil), respectively.

Human urine sample handling was approved by the ethics committee of the Federal University of Alfenas (registration number 18026513.8.0000.5142). The methodology was developed using pool urine samples ($n = 5$) obtained from volunteer non-smokers, aged between 20 and 50 years, in order to offset the matrix effect in the extraction process of the urine samples. For nicotine and cotinine determination, urine samples ($n = 4$) were obtained from volunteers who reported being smokers, in the same age group. All samples were centrifuged for 10 min at 10 000 m s^{-2}, and directly submitted to extraction by MMIPs.

Apparatus

The MMIP synthesis was performed using an ultrasonic bath (model USC2800A, Unique, São Paulo, Brazil), a heater plate (model NT103, Novatécnica, São Paulo, Brazil), a mechanical stirrer (model TE-099 Unidade Potter, Tecnal, São Paulo, Brazil), a double boiler (Frigomix B) coupled with a thermostat (Thermomix BM) (B. Braun Biotech International, Melsungen, Germany), a tube shaker (Glas-Col, Washington, USA) and a vacuum drying oven (Novatécnica, São Paulo, Brazil). The extractions were processed with a tube shaker (Vibrax VXR basic, IKA, São Paulo, Brazil) and a ferromagnetic magnet. The chromatographic analyses were performed using a Shimadzu GC-2010 gas chromatograph coupled to a mass spectrometer (GC-MS) and an AOC 20i+s autoinjector (Shimadzu®, Kyoto, Japan). The MMP was characterized by Fourier transform infrared spectrometry – FT-IR (model IS50, Thermo Scientific, Waltham, USA), thermogravimetric analysis – TGA (model SDT Q600, TA Instruments, New Castle, USA), scanning electron microscopy/energy dispersive X-ray spectrometry – SEM/EDS (model LV-JSM 6360, JEOL, Tokyo, Japan) and atomic force microscopy – AFM (NanoScope IIIa, Vecco Instruments, New York, USA).

Synthesis of the MMIP

The MMIP was synthesized in four steps. Initially, the Fe_3O_4 nanoparticles were prepared by the coprecipitation method according to Chen *et al.*[27] Thus, 15 mmol of $FeCl_3 \cdot 6H_2O$ and 10 mmol of $FeCl_2 \cdot 4H_2O$ were dissolved in 80 mL of deionized water preheated to 80 °C, under nitrogen gas and vigorous stirring. So, 50 mL of 28% (v/v) ammonium hydroxide solution was dropwise added into the solution that changed its color from clear yellow to black. The mixture was allowed to stand at 80 °C for 30 min. The obtained black precipitate (Fe_3O_4 nanoparticles) was collected by using an external magnet and washed repeatedly with deionized water until the used washing solution showed pH from 6.5 to 7.5. Finally, the particles were dried under vacuum at 60 °C for 24 h.

In the second step, the surface of Fe_3O_4 nanoparticles was modified with SiO_2 according to a study by Zeng *et al.*,[16] resulting in Fe_3O_4@SiO_2. Then, 600 mg of Fe_3O_4 nanoparticles was added into 60 mL of isopropanol : ultra-pure water (5 : 1, v/v), and the suspension was maintained in the ultrasonic bath for 20 min. Afterwards, 10 mL of 28% (v/v) ammonium hydroxide solution and 4 mL of TEOS were added promptly,

 This journal is © The Royal Society of Chemistry 2015

Published on 22 September 2015. Downloaded by Michigan State University on 21/01/2016 07:20:08.

where the reaction was maintained at room temperature with continuous stirring for 12 h. Following this, the modified magnetic nanoparticles were separated by using an external magnet, washed repeatedly with deionized water until the used washing solution showed pH from 6.5 to 7.5. Finally, the particles were dried under vacuum at 60 °C for 24 h.

In the third step, the Fe_3O_4@SiO_2 particles were functionalized with polymerizable double bonds according to Kong *et al.*,[28] resulting in vinyl-modified Fe_3O_4@SiO_2. Therefore, 200 mg of Fe_3O_4@SiO_2 was dispersed in 50 mL of methanol by sonication for 30 min. Then, 3 mL of MPS was added drop by drop under vigorous stirring. The reaction was maintained for 48 h at room temperature and with continuous stirring. The resultant product was collected by using an external magnet, rinsed with methanol several times until the supernatant became clearer then dried under vacuum at 60 °C for 24 h.

In the last step, the MIP was synthesized (by the precipitation polymerization method) over the vinyl-modified Fe_3O_4@SiO_2, resulting in the MMIPs. Thus, 0.4 mmol of nicotine (template) and 2.0 mmol of MAA (functional monomer) were dissolved in 20 mL of acetonitrile, while 489 mg of vinyl-modified Fe_3O_4@SiO_2 nanoparticles was added into another flask containing 20 mL of acetonitrile. Then, both flasks were placed simultaneously in the ultrasonic bath for 1 h to form the template–monomer complex and magnetic nanoparticle dispersion, respectively. Subsequently, the template–monomer complex was poured into the magnetic nanoparticle dispersion, and 12.0 mmol of EGDMA (cross-linker) and 80 mg of ABCVA (initiator) were immediately added into the mixture under vigorous stirring. The mixture was degassed in an ultrasonic bath for 30 min and bubbled with nitrogen gas for 15 min to remove the oxygen. The flask was sealed and the polymerization was performed at 75 °C under mechanical stirring for 24 h. The MMIPs were collected magnetically, washed sequentially with methanol : acetic acid solution (9 : 1, v/v) and pure methanol to remove the template and other reagents remaining from the synthesis. Finally, the particles were dried under vacuum at 60 °C for 24 h.

Characterization

The morphology of the materials was investigated using SEM and AFM. The encapsulation efficiency of the microspheres was measured by FT-IR, EDS and TGA.

The infrared spectra were recorded on a FT-IR spectrometer performed in attenuated total reflectance (ATR) mode in a wavelength range of 4000–400 cm^{-1}. TGA was performed starting from room temperature to 800 °C, with a heating rate of 10 °C min^{-1} and with a nitrogen flow of 100 mL min^{-1}. For SEM/EDS analyses, the samples were previously coated with a thin layer of platinum and the microscopy operated at an acceleration voltage of 15 kV. For AFM analyses, sample dispersion droplets were dried on top of freshly cleaved mica surfaces and glued to the instrument sample holder. The analyses were carried out employing a magnetic tip (silicon coated with cobalt), a resonance frequency of 75 kHz and a constant pressure of 2.8 N m^{-1}.

Extraction procedure

Twenty milligrams of the MMIP was added into a test tube containing 2.0 mL of a urine sample. The tube was vortexed for 20 min. Then, the MMIP particles were separated by using an external magnet and the urine sample was discarded. Therefore, the analytes were eluted from the MMIP using a mixture of 3.0 mL of pure methanol and 25 μL of 0.1 mol L^{-1} HCl aqueous solution, and stirred vigorously for 20 min. Afterwards, 2.7 mL of the supernatant was transferred into another test tube, and evaporated to dryness under vacuum at 60 °C. Finally, the residues were dissolved in 200 μL of pure methanol and analyzed by GC-MS.

Chromatographic conditions

Nicotine and cotinine were analyzed by GC-MS, using a RTX5-MS column (30 m × 0.25 mm i.d.; 0.25 μm film thickness) with helium as the carrier gas at a flow rate of 1.6 mL min^{-1}. Two microliters was injected in the splitless mode, at 250 °C (injector temperature). The oven temperature was programmed from 120 to 280 °C at 40 °C min^{-1}, and maintained at 280 °C for 4 min. The interface temperature was set at 280 °C and the ion source was operated in the electron ionization mode (EI; 70 eV, 250 °C). Full-scan mass spectra (m/z from 40 to 200) were recorded for both analyte identifications. Selective ion monitoring (SIM) mode was used in the quantitative analyses. The ions at m/z 162, 84 and 133 and m/z 176, 147 and 98 were used to monitor nicotine and cotinine, respectively. The quantification was based on the peak area integration at m/z 84 and 98 for nicotine and cotinine, respectively. The other ions served as qualifying ions. The total separation time was 8.0 min.

Validation

The linearity study was performed by analyzing the urine samples ($n = 5$) fortified with standard solutions of nicotine and cotinine at concentrations of 0.1, 0.5, 1.0, 2.0 and 3.0 mg L^{-1}. The limits of quantification (LOQs) were defined as the lowest concentrations that can be analyzed with precision and accuracy. The intra- and inter-day precisions as well as accuracies were assessed using a blank urine sample ($n = 5$) fortified with both nicotine and cotinine at 0.1, 1.0 and 3.0 mg L^{-1} concentrations. The recoveries were obtained by comparing the analytical signals of the extracted samples with the analytical signals of mixed nicotine and cotinine standard solutions, analyzed without extractions.

Results and discussion

Preparation of MMIPs

At first, the Fe_3O_4 nanoparticles were synthesized by the co-precipitation method for being the classical procedure for obtaining Fe_3O_4 magnetic nanoparticles, due to its simplicity and higher efficiency in terms of yield and less reaction time.[36] According to Laurent *et al.*,[36] a high concentration of iron salts used during the Fe_3O_4 synthesis can favor the nucleation stage of the nanoparticles, resulting in a more homogeneous particle size distribution. Furthermore, magnetite (Fe_3O_4) is very

Published on 22 September 2015. Downloaded by Michigan State University on 21/01/2016 07:20:08.

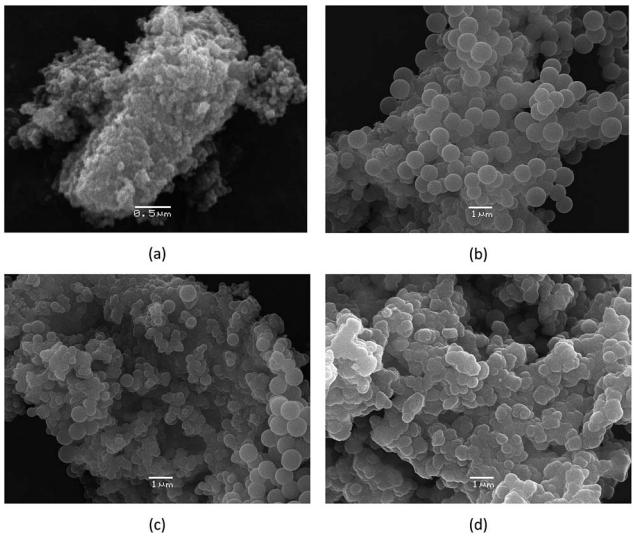

Fig. 1 SEM images of Fe_3O_4 (a), Fe_3O_4@SiO_2 (b), vinyl-modified Fe_3O_4@SiO_2 (c) and MMIP (d).

unstable, being easily oxidized to maghemite (γFe_2O_3) in the presence of oxygen and/or reacting with the excess of H^+ ions. Thus, the employment of an excess of ammonium hydroxide solution ensures a purer material production, with a minimal formation of maghemite.

The surfaces of the Fe_3O_4 nanoparticles were then coated with silica layers, reacting with TEOS. This procedure was carried out in order to prevent the oxidization and aggregation of the nanoparticles, as well as to provide them with superficial reactive silanol groups. Hence, the Fe_3O_4@SiO_2 superficial hydroxyl groups reacted with MPS to introduce vinyl groups on the surface of the nanoparticles, forming polymerizable sites. The double bonds on the surface of vinyl-modified Fe_3O_4@SiO_2 nanoparticles can react with methacrylate groups to initiate the co-polymerization of the MAA and EGDMA.

The MIP synthesis was carried out according to Figueiredo *et al.*,[37] adopting the precipitation polymerization method followed by Chen *et al.*[27] Then, the MAA and EGDMA were chosen, respectively, as the functional monomer and cross-linker, as in Figueiredo's work. A racemic mixture of nicotine was used as the template molecule, since smokers are exposed to both enantiomers of nicotine, due to pyrolytic racemization of the *S*-(−)-isomer during smoking.[38] In this way, the synthesized MIP is endowed with selective sites for both enantiomeric forms of nicotine. According to the literature, the functional monomer should be employed in a higher amount in relation to the template molecule in order to displace the equilibrium towards the formation of the template–monomer complex.[39] Furthermore, the cross-linker should be present in excess over the functional monomer to provide greater mechanical stability and appropriate porosity to the polymer.[6] So, an optimum molar ratio of 1 : 5 : 30 (template : MAA : EGDMA) was employed according to the results obtained by Chen *et al.*[27]

The MMIP was used to extract nicotine and cotinine directly from untreated urine samples, which normally present pHs within 5.0 and 7.0. In this pH range, the pyrrolidine ($pk_a = 8.2$) and pyridine ($pk_a = 3.1$) rings were positively ionized and non-ionized,

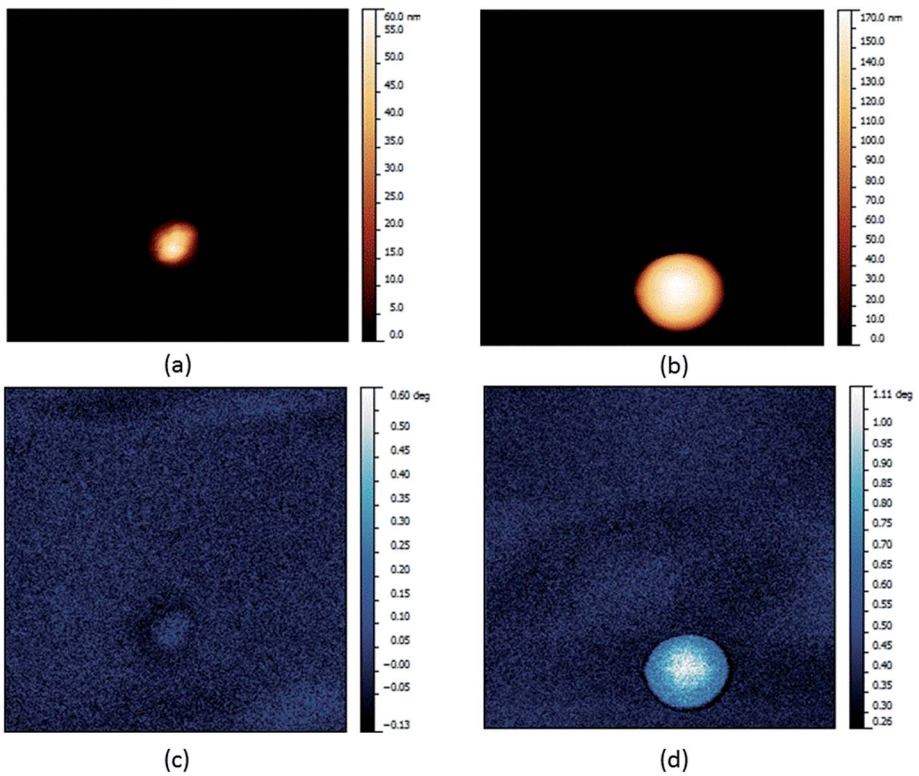

Fig. 2 AFM images: topography of Fe_3O_4 (a) and Fe_3O_4@SiO_2 (b); magnetic force microscopy (MFM) of Fe_3O_4 (c) and Fe_3O_4@SiO_2 (d).

 This journal is © The Royal Society of Chemistry 2015

Published on 22 September 2015. Downloaded by Michigan State University on 21/01/2016 07:20:08.

respectively, whereas the carboxyl group ($pk_a = 4.7$) of the MAA was negatively ionized. Thus, the binding mechanism of the MMIP was based on the electrostatic interaction between the pyrrolidinyl groups of nicotine/cotinine with the carboxyl group of the MAA.[37]

Characterization

The morphologies of the Fe_3O_4, Fe_3O_4@SiO_2, vinyl-modified Fe_3O_4@SiO_2 and MMIP were investigated by SEM (Fig. 1). It was not possible to observe the shape of the Fe_3O_4 nanoparticles, probably due to the particle aggregations as well as the low-resolution of the micrographs (Fig. 1a). However, it can be clearly seen that Fe_3O_4@SiO_2 and vinyl-modified Fe_3O_4@SiO_2 are regular spheres (Fig. 1b and c, respectively), with particle sizes ranging from a few nanometers to about 1 μm. Despite having a low resolution, the MMIP micrograph (Fig. 1d) indicated that these particles are also spherical and aggregated as cluster forms.

The Fe_3O_4 and Fe_3O_4@SiO_2 nanoparticles were isolated and analyzed by topography and magnetic force microscopy (Fig. 2). The larger diameter of the Fe_3O_4@SiO_2 particles is probably due to the presence of the TEOS layer. The magnetic force intensity is low and homogeneously distributed throughout the Fe_2O_3 nanoparticle, probably due to its reduced size. However, a more intense magnetic force (clear color) could be observed in the core of the Fe_3O_4@SiO_2 nanoparticles (Fig. 2d) compared to its edges (dark color). This result can be explained by the fact that the magnetic tip is sensitive to the magnetic and electrical fields. Thus, in the core there is an association of the magnetic forces of the Fe_2O_3 nanoparticles with the electrical forces of the chemical groups of the TEOS, whereas in the edges there is only the electrical force.

In the FT-IR spectra, the absorption band at about 580 cm^{-1} was characteristic of the Fe–O vibration (Fig. 3a). The bands at 800, 950 and 1070 cm^{-1} in Fe_3O_4@SiO_2 and vinyl-modified Fe_3O_4@SiO_2 FT-IR spectra (Fig. 3b and c, respectively) were attributed to the stretching of Si–O, Si–O–H and Si–O–Si, respectively, confirming that the Fe_3O_4 nanoparticles were adequately coated with TEOS and MPS. The MMIPs displayed a strong absorption band at about 1735 cm^{-1} (characteristic of the ester C=O vibration) and less intense absorption bands at 1386 and 1251 cm^{-1} (characteristic of the ester C–O vibration) attributed to EGDMA. Moreover, the bands at 2924 and 2852 cm^{-1} corresponded to the symmetrical and asymmetrical stretching of the sp^3 carbon C–H bond. They also confirmed the presence of the polymeric layer on the magnetic nanoparticle surfaces.

TGA was performed to attest the encapsulation efficiency of the magnetic nanoparticles as well as to establish the thermal stability of the materials. According to Fig. 4, the less weight loss, in all the samples, at temperatures less than 200 °C was attributed to water evaporation. A minimal weight loss (about 4.5%) was observed for the Fe_3O_4 nanoparticles heated to 800 °C due to their inorganic nature. Besides water loss, the Fe_3O_4@SiO_2 and vinyl-modified Fe_3O_4@SiO_2 nanoparticles demonstrated a weight loss of about 2.86 and 3.15%, respectively, when heated from 200 to 800 °C. In the case of the Fe_3O_4@SiO_2 nanoparticles, this result may be due to the hydroxyl group condensations and/or residual ethoxide group degradations, while for vinyl-modified Fe_3O_4@SiO_2 this weight loss probably was a result of the grafted MPS decomposition. Finally, the MMIP showed a greater weight loss (about 70.94%) compared to the other materials, which ensured the presence of an organic network.

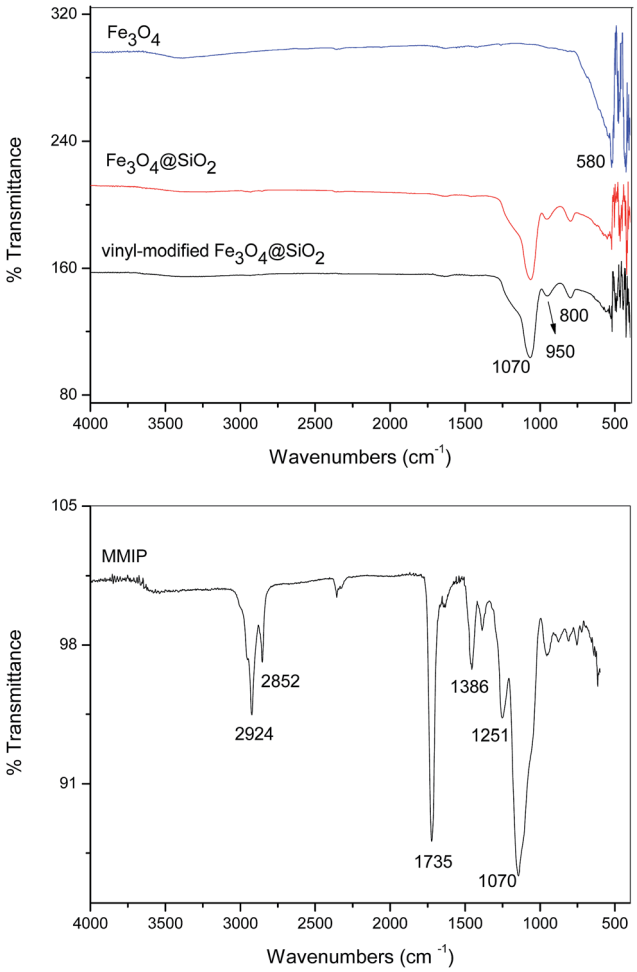

Fig. 3 FTIR spectra of the Fe_3O_4, Fe_3O_4@SiO_2, vinyl-modified Fe_3O_4@SiO_2 and MMIP.

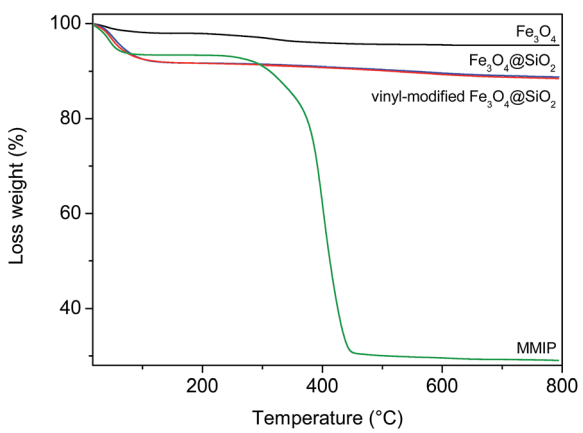

Fig. 4 TGA curves of the Fe_3O_4, Fe_3O_4@SiO_2, vinyl-modified Fe_3O_4@SiO_2 and MMIP at a heating rate of 10 °C min^{-1} from 17 °C to 800 °C in a nitrogen flow (100 mL min^{-1}).

Published on 22 September 2015. Downloaded by Michigan State University on 21/01/2016 07:20:08.

Table 1 Elemental composition of the materials obtained by EDS analyses

Element	Fe_3O_4	Fe_3O_4@SiO_2	Vinyl-modified Fe_3O_4@SiO_2	MMIP
C	11.24	41.62	56.46	74.44
O	27.02	35.77	29.29	15.02
Si	—	10.60	6.27	4.02
Fe	54.02	4.79	3.54	2.40
Zn[a]	—	0.38	0.48	0.39
Cu[b]	0.72	0.86	0.49	0.42
Pt[c]	7.00	5.98	3.48	3.31
Total	100.00	100.00	100.00	100.00

[a] Impurities. [b] Impurities. [c] Platinum coating required to perform the SEM/EDS analyses.

Table 1 shows the chemical composition obtained by EDS for all the materials. The small amount of platinum in all samples is due to the platinum coating required to perform the analyses. For the Fe_3O_4 nanoparticles, the presence of iron and oxygen atoms was observed in a large proportion as well as a small amount of carbon, which is probably due to some contamination. For the Fe_3O_4@SiO_2 nanoparticles, there was a reduction in the iron percentage and an increase in the oxygen percentage, besides a large amount of silicon, which proves that they were coated with TEOS. Furthermore, it is important to note a considerable amount of carbon (41.62%) in the Fe_3O_4@SiO_2 nanoparticles, which can be attributed to the presence of residual ethoxide groups on the particle surface. Likewise, the functionalization with MPS can be confirmed by the high carbon percentage in the vinyl-modified Fe_3O_4@SiO_2 nanoparticles. Although MPS contains silicon and oxygen in its chemical structure, the percentage of these atoms decreased probably because there was an increase in the carbon percentage (which now represents more than 50% of the sample). Finally, the polymerization on the magnetic nanoparticle surfaces can be attested since there was an increase in the carbon percentage as well as a reduction in the other constituents (*e.g.* oxygen, silicon and iron) in the MMIP sample. It is noteworthy that the presence of copper and zinc in very small quantities comes from impurities.

Figures of merit

The mass spectra of nicotine and cotinine obtained by SCAN analysis are shown in Fig. 5. The most intense peaks for nicotine were at *m*/*z* 84 (base peak), 133 and 162 (molecular peak),

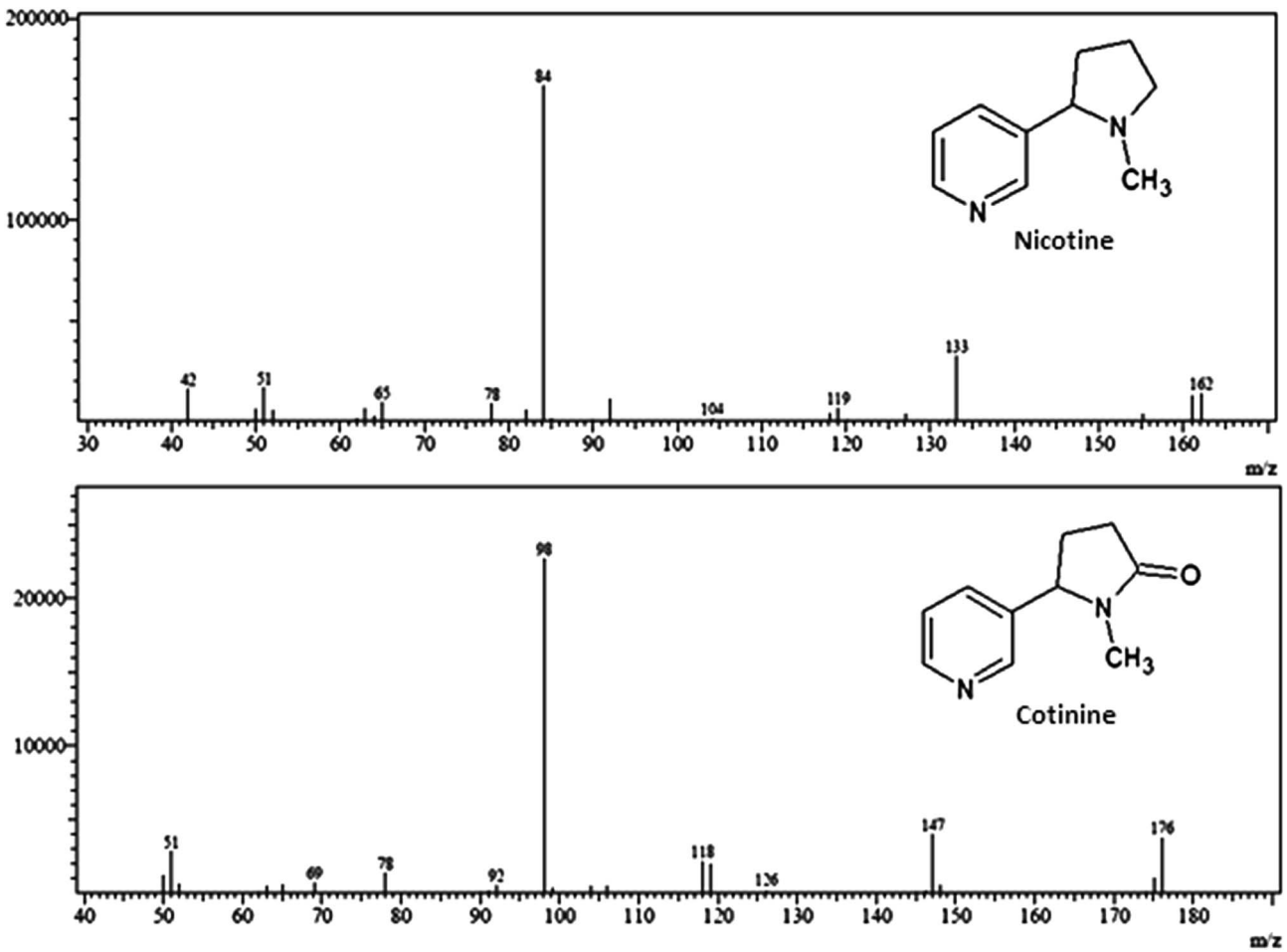

Fig. 5 Mass spectra of nicotine and cotinine.

 This journal is © The Royal Society of Chemistry 2015

Published on 22 September 2015. Downloaded by Michigan State University on 21/01/2016 07:20:08.

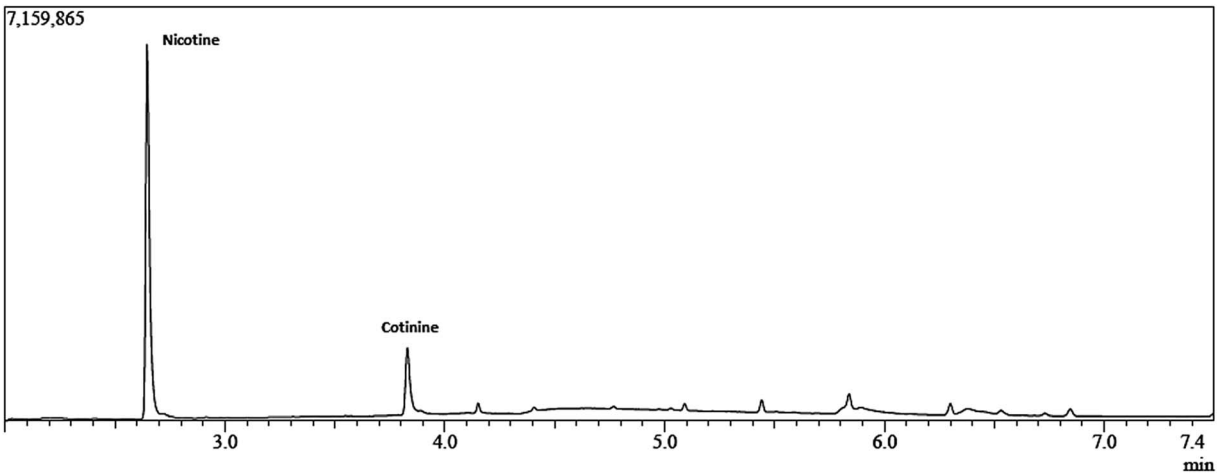

Fig. 6 Chromatogram of a urine sample from a non-smoker fortified with 3.0 mg L^{-1} of nicotine and cotinine.

whereas for cotinine, they were at *m*/*z* 98 (base peak), 147 and 176 (molecular peak). Therefore, the runs were performed in the SIM mode in order to increase the method's sensitivity and selectivity. The SIM chromatogram of an extracted urine sample spiked with 3 mg L^{-1} of nicotine and cotinine is shown in Fig. 6. As it can be seen, the chromatogram contains few interferents, confirming the MMIP selectivity for the analytes. Furthermore, for the same concentration of the analytes, the MMIP extracted significantly more nicotine than cotinine (Fig. 6). This confirms the selectivity of the MMIP since nicotine was used as the template molecule. As cotinine has a very similar structure to nicotine, it was also extracted but in a lower proportion. Additionally, it is important to point out that the MMIP synthesis was very similar (in terms of template, functional monomers and cross linker proportion) to the synthesis of a MIP selective to nicotine in our previous publication,[37] and it was possible to conclude that the MIP was really more selective to nicotine, in comparison with cotinine, anabasine, nornicotine, and caffeine.

The evaluated validation parameters were linearity, limit of quantification, precision and accuracy. For this purpose, we used a urine pool obtained by mixing five samples from non-smokers, in order to offset the effect of the matrix in extraction processes of the urine samples. The method was linear for both analytes in the range from 0.1 to 3.0 mg L^{-1}, with correlation coefficients larger than 0.99 (for both analytes). The regression equations were $Y = 2\,496\,212X - 33\,541$ and $Y = 551\,186X + 8556$ for nicotine and cotinine, respectively, where X is the concentration of the studied compounds and Y is the peak area. The limit of quantitation (LOQ) for both analytes was 0.1 mg L^{-1}. The intra- and inter-day precision and accuracy (Table 2) are in accordance with the FDA recommendations.[40] All the results showed that the proposed method was sufficiently accurate, selective and simple for the determination of nicotine and cotinine in human urine samples.

Application to real samples

Under the optimized conditions, the proposed method was applied to analyze four smokers' urine samples (in triplicate).

Table 2 Precision and accuracy for nicotine and cotinine extracted from urine by the MMIP

		Nicotine			Cotinine		
Intra-day	NC[a]/mg L^{-1}	0.10	1.00	3.00	0.10	1.00	3.00
	OC[b]/mg L^{-1}	0.10	1.02	3.15	0.09	1.06	3.16
	Precision[c]/%	7.85	7.47	9.68	19.63	4.81	14.20
	Accuracy[d]/%	4.09	1.90	4.93	−4.86	6.14	5.39
Inter-day	NC[a]/mg L^{-1}	0.10	1.00	3.00	0.10	1.00	3.00
	OC[b]/mg L^{-1}	0.11	0.94	2.77	0.10	0.91	2.88
	Precision[c]/%	12.55	10.01	13.45	8.62	14.28	8.41
	Accuracy[d]/%	7.85	−6.37	−7.74	2.71	−8.88	−3.97

[a] Nominal concentration. [b] Obtained concentration. [c] As relative standard deviation. [d] As a relative error.

Nicotine was detected in all the samples, but in concentrations lower than the LOQ, whereas cotinine concentrations ranged from 0.191 to 0.276 mg L^{-1}. These results can be explained by the short half-life of nicotine (about 2 h (ref. 33)), and by the fact that the urine samples were collected in the morning. Thus, as already affirmed by the literature,[41] nicotine was not a suitable biomarker. On the other hand, the proposed method was suitable for monitoring exposure to tobacco, since cotinine is the most used biomarker for tobacco exposure, having a long half-life of about 20 h and being excreted in greater amounts in the urine. Furthermore, 0.1 mg L^{-1} urinary cotinine is known as a cut-off for active smokers.[42]

Conclusions

In this study, a MMIP for nicotine and cotinine extraction from urine samples was successfully prepared and characterized. The obtained MMIP was easily collected using an external magnetic field, without any additional centrifugation or filtration step, avoiding the use of packed columns/cartridges, like in the conventional SPE. The extraction procedure was fast, simple and efficient. The MMIP was adequately used to extract nicotine and cotinine directly from real human urine samples followed

Published on 22 September 2015. Downloaded by Michigan State University on 21/01/2016 07:20:08.

by GC-MS analyses, where some advantages can be emphasized, like good selectivity, sensitivity, reproducibility and analytical frequency. Thus, we believe that the method can be easily applied to monitoring tobacco exposure.

Acknowledgements

We thank the "Fundação de Amparo à Pesquisa do Estado de Minas Gerais" (FAPEMIG, Belo Horizonte, Brazil), Project CDS-APQ-01612-10, "Conselho Nacional de Desenvolvimento Científico e Tecnológico" (CNPq, Brasília, Brazil), Project 483371/2012-2 and Coordenação de Aperfeiçoamento de Pessoal Nível Superior (CAPES) for their financial support. We also thank the National Center for Research in Energy and Materials (CNPEM) and Chemistry Institute of Unicamp for the AFM and SEM analyses, respectively.

References

1 J. D. Winefordner, *Sample Preparation Techniques in Analytical Chemistry*, John Wiley & Sons, Inc., Hoboken, New Jersey, 2003.
2 Y. Chen, Z. Guo, X. Wang and C. Qiu, *J. Chromatogr. A*, 2008, **1184**, 191–219.
3 C. He, Y. Long, J. Pan, K. Li and F. Liu, *J. Biochem. Biophys. Methods*, 2007, **70**, 133–150.
4 V. Pichon, *J. Chromatogr. A*, 2007, **1152**, 41–53.
5 L. I. Andersson, *J. Chromatogr., Biomed. Appl.*, 2000, **745**, 3–13.
6 D. A. Spivak, *Adv. Drug Delivery Rev.*, 2005, **57**, 1779–1794.
7 L. Chen and B. Li, *Anal. Methods*, 2012, **4**, 2613–2621.
8 E. Benito-Pena, S. Martins, G. Orellana and M. C. Moreno-Bondi, *Anal. Bioanal. Chem.*, 2009, **393**, 235–245.
9 L. Chen, J. Liu, Q. Zeng, H. Wang, A. Yu, H. Zhang and L. Ding, *J. Chromatogr. A*, 2009, **1216**, 3710–3719.
10 X. Hu, J. Pan, Y. Hu, Y. Huo and G. Li, *J. Chromatogr. A*, 2008, **1188**, 97–107.
11 E. Caro, R. M. Marce, P. A. G. Cormack, D. C. Sherrington and F. Borrull, *Anal. Chim. Acta*, 2005, **552**, 81–86.
12 Z. Zhang, W. Tan, Y. Hu and G. Li, *J. Chromatogr. A*, 2011, **1218**, 4275–4283.
13 I. Mendiara, C. Domeño and C. Nerín, *J. Sep. Sci.*, 2012, **35**, 3308–3316.
14 I. Mendiara, K. Bentayeb, C. Nerín and C. Domeño, *Talanta*, 2015, **132**, 690–697.
15 F.-F. Chen, X.-Y. Xie and Y.-P. Shi, *Talanta*, 2013, **115**, 482–489.
16 H. Zeng, Y. Z. Wang, C. Nie, J. H. Kong and X. J. Liu, *Analyst*, 2012, **137**, 2503–2512.
17 W. Li, L. Yang, F. Wang, H. Zhou, X. Yang, Y. Huang and H. Liu, *Biochem. Eng. J.*, 2013, **79**, 206–213.
18 S. Shi, J. Guo, Q. You, X. Chen and Y. Zhang, *Chem. Eng. J.*, 2014, **243**, 485–493.
19 Y. Hiratsuka, N. Funaya, H. Matsunaga and J. Haginaka, *J. Pharm. Biomed. Anal.*, 2013, **75**, 180–185.
20 Y.-L. Zhang, J. Zhang, C.-M. Dai, X.-F. Zhou and S.-G. Liu, *Carbohydr. Polym.*, 2013, **97**, 809–816.
21 T. Jing, H. Xia, Q. Guan, W. Lu, Q. Dai, J. Niu, J.-M. Lim, Q. Hao, Y.-I. Lee, Y. Zhou and S. Mei, *Anal. Chim. Acta*, 2011, **692**, 73–79.
22 M. Bouri, M. J. L-García, R. Salghi, M. Zougagh and A. Ríos, *Talanta*, 2012, **99**, 897–903.
23 G. Ma and L. Chen, *J. Chromatogr. A*, 2014, **1329**, 1–9.
24 L. Chen and B. Li, *Food Chem.*, 2013, **141**, 23–28.
25 C. Hu, J. Deng, Y. Zhao, L. Xia, K. Huang, S. Ju and N. Xiao, *Food Chem.*, 2014, **158**, 366–373.
26 D. He, X. Zhang, B. Gao, L. Wang, Q. Zhao, H. Chen, H. Wang and C. Zhao, *Food Control*, 2014, **36**, 36–41.
27 F.-F. Chen, X.-Y. Xie and Y.-P. Shi, *J. Chromatogr. A*, 2013, **1300**, 112–118.
28 X. Kong, R. Gao, X. He, L. Chen and Y. Zhang, *J. Chromatogr. A*, 2012, **1245**, 8–16.
29 Y. Zhang, R. Liu, Y. Hu and G. Li, *Anal. Chem.*, 2009, **81**, 967–976.
30 Y. Zhang, Y. Li, Y. Hu, G. Li and Y. Chen, *J. Chromatogr. A*, 2010, **1217**, 7337–7344.
31 Y. Hu, Y. Li, R. Liu, W. Tan and G. Li, *Talanta*, 2011, **84**, 462–470.
32 G. M. Lackmann, U. Salzberger, U. Tollner, M. Chen, S. G. Carmella and S. S. Hecht, *J. Natl. Cancer Inst.*, 1999, **91**, 459–465.
33 S. Oga, *Fundamentos de Toxicologia*, Ateneu, São Paulo, 3rd edn, 2008.
34 H. Kataoka, R. Inoue, K. Yagi and K. Saito, *J. Pharm. Biomed. Anal.*, 2009, **49**, 108–114.
35 J. B. Patel, S. N. Shukla, H. R. H. Patel, K. K. Kothari, P. M. Shah and P. S. Patel, *Asian Pacific J. Cancer Prevention*, 2007, **8**, 229–235.
36 S. Laurent, D. Forge, M. Port, A. Roch, C. Robic, L. V. Elst and R. N. Muller, *Chem. Rev.*, 2008, **108**, 2064–2110.
37 E. C. Figueiredo, D. M. de Oliveira, M. E. P. B. de Siqueira and M. A. Z. Arruda, *Anal. Chim. Acta*, 2009, **635**, 102–107.
38 S. Kodama, A. Morikawa, K. Nakagomi, A. Yamamoto, A. Sato, K. Suzuki, T. Yamashita, T. Kemmei and A. Taga, *Electrophoresis*, 2009, **30**, 349–356.
39 X. Shi, A. Wu, G. Qu, R. Li and D. Zhang, *Biomaterials*, 2007, **28**, 3741–3749.
40 Guidance for Industry, Bioanalytical Method Validation, U.S. Department of Health and Human Services Food and Drug Administration, Center for Drug Evaluation and Research (CDER), Center for Veterinary Medicine (CVM), May 2001, http://www.fda.gov/downloads/Drugs/Guidances/ucm070107.pdf.
41 C. N. Man, L.-H. Gam, S. Ismail, R. Lajis and R. Awang, *J. Chromatogr. B: Anal. Technol. Biomed. Life Sci.*, 2006, **844**, 322–327.
42 T. Tapani, J. Tom and R. Kari, *Clin. Chem.*, 1999, **45**, 2164–2172.

 This journal is © The Royal Society of Chemistry 2015